



Performance Enforcement of a Parabolic Solar Collector with a Separating Transparent Glass Sheet

S. A. Gandjalikhan Nassab*

Department of Mechanical Engineering, Shahid Bahonar University of Kerman, Kerman, Iran

PAPER INFO

Paper history:

Received 05 January 2022

Accepted in revised form 24 March 2022

Keywords:

Compound parabolic collectors

Glass sheet

Natural convection

Performance

Turbulent

ABSTRACT

This paper deals with the development of compound parabolic collectors (CPCs), utilizing a partial glass sheet adjacent to the absorber plate for the purpose of performance improvement. The collector under study has a parabolic shape, whose cavity is filled with air and the turbulent natural convection takes place because of the air density gradient. The main goal is the reduction of heat losses by keeping away the high-temperature region near to the absorber from the main recirculated convection airflow by installation of a separating glass sheet. The conservations of mass, momentum and energy as the set of governing equations for the steady and turbulent free convection airflow in the CPC's cavity and the Laplace equation for computation of temperature distributions in solid parts including the glass cover, absorber plate, and glass sheet were numerically solved by the finite element method. The COMSOL Multiphysics software was used for the present simulation. For the computation of turbulent stress and heat flux, the κ - ϵ turbulence model was employed. An attempt was made to investigate the installation of a fully transparent glass sheet near the absorber plate on the thermal behavior of the studied CPC. It is expected that this factor leads to lowering the heat losses from boundary surfaces, especially from the glass cover. Numerical findings showed about a 24% increase in the efficiency of studied test cases because of the installed glass sheet. Comparison between the theoretical findings with experiment shows good consistency.

doi: 10.5829/ijee.2022.13.02.07

NOMENCLATURE

		Greek Symbols	
a	Length of glass sheet (m)	α	Absorptivity (-)
b	Height of glass sheet (m)	β	Volumetric thermal expansion (1/K)
c_p	Specific heat (kJ/kg K)	ρ	Reflectivity (-)
g	Gravitational acceleration (m/s^2)	τ	Transmissivity (-)
h	Convection coefficient ($W/m^2 K$)	δ	Thickness (m)
H	Height of CPC (m)	μ	Viscosity (Pa. s)
k	Thermal conductivity ($W/m K$)	ρ	Density (kg/m^3)
L	Length (m)	ϵ	Surface radiation emissivity
p	Pressure (Pa)	ϑ	Kinematic viscosity (m^2/s)
q	Heat flux (W/m^2)	η	Efficiency (-)
T	Temperature (K)	Subscript	
T_0	Working fluid temperature (K)	abs	Absorber
(x, y)	Coordinate axes (m)	w	Wall
(u, v)	x- and y- velocity components (m/s)	amb	Ambient
(x, y)	Vertical and horizontal coordinates (m)	wf	Working fluid
V	Velocity magnitude (m/s)		

*Corresponding Author Email: ganji110@uk.ac.ir (S. A. Gandjalikhan Nassab)

INTRODUCTION

The rapid growth of global demand for energy in all industrial areas and at the same time fast depletion of fossil fuels all around the world are undeniable but hopefully have been recognized by governments and researchers as a crucial problem. Providing a sustainable remedy was soon turned into an acceptable global mission for researchers to attack this issue. Using as much renewable energy is an efficient way for this purpose. Iran has a vast potential for renewable energy and wind and solar energy resources are the best among other renewable energy resources in the region. Iran has huge solar PV potential with average solar radiation of 4.5-5.5 kWh/m² and up to 300 sunny days a year over 2/3 of its total area. The regions of highest concentration of irradiation are the central and southern areas. The maximum capacity of installed renewable energy power plants in Iran belongs to Solar (PV) power plants with 309 MW capacity. The second position is for the Wind energy power plants with 285 MW capacity [1]. So, due to the importance of using Solar energy in Iran, the higher performance of collectors that have the main role in converting radiative heat flux into other useful energies becomes the topic of many research studies.

The compound parabolic collector (CPC) is one of an efficient solar concentrator that has attracted large attention from researchers. It has naturally a low heat loss characteristic property for medium and high-temperature applications. This non-imaging concentrator has the capability of reflecting and intercepting the solar incident toward the black absorber over a wide-angle range. So, the expansive tracking systems can be avoided with a proper choice of orientation and inclination in CPCs. The additional reason of interest is the capability of accepting diffuse solar radiation.

Among all of the solar collectors, parabolic types are commonly used in many systems, such as water heating and desalination [2], drying process [3], and air conditioning (space heating) [4, 5]. Although, there are many published papers for designing high-performance collectors, however, there is a deep gap between the existing CPCs with the optimum ones and more research works are needed to reach this goal. Many proposed methods for enhancing the rate of heat transfer in CPCs have been reported in literature [6, 7].

A parametric study of airflow in CPCs has been reported by Eames et al. [8]. In that study, CPCs with various different acceptance angles and boundary conditions were simulated. The well-known stream function-vorticity method was applied in the numerical solution of the conservations of mass, momentum, and energy for free convection airflow inside the cavity of collector using triangular grids. From the numerical findings, a correlation for computation of Nusselt number as a function of Grashof number was reported. In similar

research, laminar free convection airflow in a CPC cavity was simulated by employing the finite element method (FEM) by Chew et al. [9]. In that study, the numerical results were presented for representative CPCs with tubular absorbers and the effects of Grashof number and the inclination angle on the thermal characteristics of collector were examined. It was found that higher rates of heat transfer between the absorber and the glass cover take place under high Grashof numbers and shallower cavities. Antonelli et al. [10] proposed a methodology to estimate the rate of heat losses inside CPCs by CFD method under the presence of radiative heat transfer. Numerical results were applied to describe some correlations for computation of the Nusselt number distribution on the receiver. These correlations were used to calculate the rate of heat losses from the receiver and to examine the influence of several important factors on the CPC performance.

The surface radiation and natural convection heat transfer in a solar cavity receiver were studied by Shirvan et al. [11] using the CFD technique. The numerical solutions were developed by means of the second-order upwind scheme using the SIMPLE algorithm. The effects of physical factors such as the Rayleigh number, inclination angles of the cavity walls, and the surface emissivity on combined natural convection-surface radiation heat transfer rate were analyzed. It was revealed that the solar cavity performance is much affected by the Rayleigh number and surface emissivity.

The design, development, and performance evaluation of a single-phase thermosyphon in an evacuated tube receiver integrated with a modified CPC solar collector were presented experimentally by Akhter et al. [12]. The thermohydraulic performance of the developed system was evaluated in the tropical climate using Therminol-55 oil as heat transfer fluid. The results demonstrated that the maximum outlet temperature reached over 120°C using thermal oil as heat transfer fluid, while it remained at 100°C in case of water.

A comprehensive state-of-the-art review of the CPC was presented by Jiang et al. [13], including design features, structure, applications, etc. Key design guidelines, structural improvements, and recent developments were also discussed in that work. As a main result, it was reported that there is no "perfect CPC", as the acceptance angle and the concentration ratio cannot be improved at the same time. Therefore, the most suitable CPC curve and structure form need to be chosen according to the purpose and requirements of the application.

As a new method for improving the CPC performance, using radiating gas instead of air inside the cavity of compound parabolic collectors was suggested and verified by Gandjalikhan Nassab and Moein Addini [14]. The collector under was filled with a participating working gas such as carbon dioxide. In numerical

simulation, the flow equations for the steady natural convection in the CPC's cavity and the conduction equation for glass cover and absorber plate were solved by the finite element method. The radiative transfer equation was solved by the discrete ordinate method, considering both diffuse and collimated radiations. It was observed that the gas radiation causes high temperature with a more uniform distribution inside the cavity of collector. Also, numerical results showed a more than 3% increase in the rate of heat transfer from the absorber surface into the working fluid because of the gas radiation effect.

Recently, a novel type of CPC, using a suitable selective coating was studied and examined by Ma et al. [15]. From the obtained experimental results, it was revealed that the solar collector with coating can operate at working temperatures over 373 K, while the maximum outlet temperature was measured in the range of 413–453 K during the Sunny day of experiment.

Based on the CPC configuration, the main factor of heat loss is due to the naturally airflow inside the cavity of solar collector. The free convective recirculated flow, which is in contact with the high-temperature absorber surface from below and the cold glass cover at the top of collector plays a major role in heat transfer from the thermal system into the environment. In the present study, a novel design of the CPC cavity for the purpose of lowering the rate of heat loss and having higher performance is proposed by installing a partial glass sheet adjacent to the absorber plate as depicted in Figure 1. By this technique, the high-temperature absorber is kept away from the main convection airflow and a lower rate of heat loss is expected. To examine this technique, the flow equations including the conservations of mass, momentum, and energy for turbulent natural convection airflow and the conduction equation for the solid elements are solved by the FEM using the COMSOL Multiphysics. Finally, the effect of a fully transparent glass sheet with different lengths on the thermal performance of CPC was thoroughly explored.

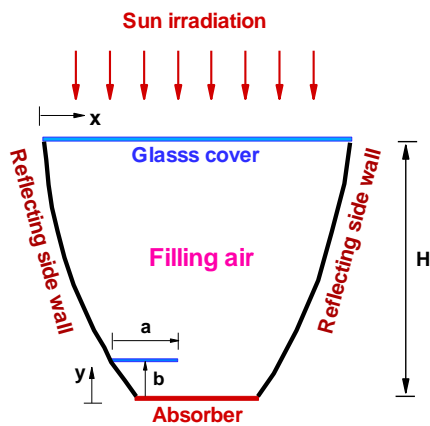


Figure 1. Geometry of the studied CPC

DESCRIPTION OF THE MODEL

A schematic of the analyzed CPC is shown in Figure 1. The collector was assumed to be made of glass for the cover and the separating sheet, polystyrene for the insulation and copper for the receiver. The air in the cavity is considered as an incompressible ideal gas. All of the physical properties of solid elements are summarized in Table 1. Grashof number defined as $Gr = g\beta\Delta TL^3/\nu\alpha$ is about 10^{10} corresponds to turbulent naturally flow.

The compound parabolic solar collectors as non imaging concentrators have the capability of reflecting all of the incident radiation on the aperture and within the acceptance angle toward the absorber plate. A small part of the incoming solar heat flux equal to $\alpha_{glass} \cdot q_{Sun}$ is absorbed by the glass cover and most of this radiative beam is transmitted by this element. Since, the applied glass sheet is very thin (with 2mm thickness), its radiant absorption was ignored in simulation and this element was considered to be quite transparent against the short wave solar irradiation. The lower absorber surface is in contact with the convective flow of working fluid at a temperature of 350 K and convection coefficient of $h = 20 W/m^2K$. The outer boundary surfaces of the reflecting walls and glass cover were assumed in convection heat transfer with $T_{amb} = 293 K$. All of the air thermo-physical properties were supposed to be temperature-dependent, while the variation of air density with temperature was determined by Boussinesq approximation. It should be recalled that the height of glass sheet installation which is $b = 60 mm$, is determined iteratively for having the best performance.

CPCs as non-imaging concentrators can be ideal or truncated. The ideal CPCs have the maximum concentration ratio, i.e. $C_r = A_{Aperture}/A_{receiver}$, while

Table 1. The parameters' values for the collector

Parameter	Value	Parameter	Value
δ_{cover}	6 mm	δ_{abs}	10 mm
ϵ_{cover}	0.9	ϵ_{abs}	0.95
α_{cover}	0.05	ρ_{cover}	0.05
τ_{cover}	0.9	T_{amb}	293 K
k_{cover}	0.78 W/m K	L_{abs}	0.25 m
k_{abs}	300 W/m K	L_{cover}	0.55 m
H	0.55 m	q_{Sun}	1100 W/m ²
ρ_{wall}	0.85	T_{abs}	340 K
a	0- 0.3 m	b	60 mm
δ_{glas}	2 mm	T_{wf}	350 K
C_r	1.63	h_{wf}	20 W/m ² K

this parameter for truncated one is $C_r = 1/\sin\theta_c$ (Figure 2). The analyzed CPC in the present work is a truncated collector with a concentration ratio of 1.63.

GOVERNING EQUATIONS AND BOUNDARY CONDITIONS

All of the flow equations for turbulent free convection airflow inside the CPC’s cavity and also the conduction equation for all solid elements may be expressed in a tensor notation as follows:

$$\nabla \cdot (\rho \vec{U} \varphi) = \nabla \cdot (\Gamma_\varphi \nabla \varphi) + S_\varphi \tag{1}$$

In Equation (1), the dependent variable, φ , stands for the x- and y-velocity components, temperature, turbulent kinetic energy and its dissipation rate. Whereas S_φ and Γ_φ represent the source terms and diffusion coefficients, respectively. The particular expressions for each dependent variable and also about Γ_φ and S_φ with some details are given in literature [16]. In computation of the turbulent stress and heat flux inside the airflow, the standard $k - \epsilon$ model along with the RANS method was used [17, 18].

In the numerical solution of Equation (1), the required boundary conditions can be stated as follows:

- No slip condition is employed in velocity computation.
- On the absorber surface, a constant heat flux $C_r \times q_{sun} \times \tau_{cover}$ (W/m^2) due to the incoming solar beam is imposed.
- The following conjugate boundary condition, which is based on the continuity of temperature and heat flux is employed at the air-solid interfaces:

$$\left[-k_{th} \frac{\partial T}{\partial n}\right]_{solid} = \left[-k_{th} \frac{\partial T}{\partial n}\right]_{air} \tag{2-a}$$

$$T_{solid} = T_{air} \tag{2-b}$$

- The convection boundary condition with its equivalent convection coefficient on the outer surface of glass cover is applied based on the following relations [19]:

$$h = h_{conv} + h_{rad} \tag{3}$$

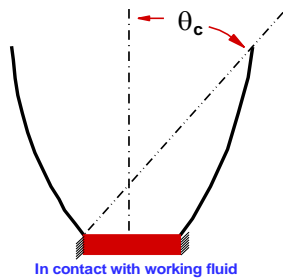


Figure 2. The acceptance angle of a truncated CPC

$$h_{conv} = 5.7 + 3.8V_{wind} \tag{4}$$

$$h_{rad} = \sigma \epsilon \left(\frac{T_{cover}^4 - T_{sky}^4}{T_{cover} - T_{amb}} \right) \tag{5}$$

where

$$T_{sky} = 0.0522T_{amb}^4 \tag{6}$$

It should be mentioned that the same boundary condition is imposed on the outer surfaces of the side walls.

Grid study

The grid study that leads to the optimum grid size must be provided in each CFD simulation. For this purpose, the maximum temperature inside the CPC was selected as the checkpoint, because it was very sensitive to mesh size. The values of maximum temperature at the different numbers of elements were calculated and are presented in Table 2. The precision of numerical findings was set equal to 1% and accordingly, the discretized computational domain with 8440 elements has been selected in all of the subsequent simulations.

Because the existence of curved boundaries, the unstructured triangular grid was used as shown in Figure 3; such that near the interface boundaries, the mesh size was refined.

Validation

The numerical result was validated first with the experimental findings reported by Cheesewright et al. [20]. In that study, the turbulent free convection airflow in a tall cavity was investigated. The velocity distribution

Table 2. Converged solutions at different grid sizes

Elements number	$T_{max}(K)$	Error respect to previous step
2520	381.6	-
2520	381.6	6%
2520	381.6	3.5%
2520	381.6	1%
2520	381.6	0.5%

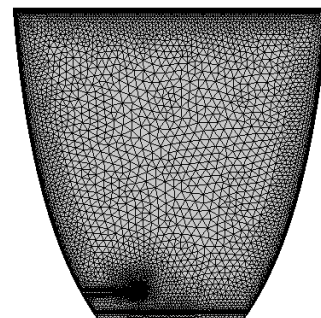


Figure 3. The unstructured triangular mesh

of airflow at the horizontal mid-plane of cavity based of the present numerical analysis is plotted in Figure 4. A comparative analysis was made with the experiment. This figure shows an almost stagnant region in the central zone of cavity and high velocity near to the cold and hot sidewalls due to the buoyancy. As shown, there is a good and acceptable agreement between the present simulation and experimental results reported by Cheesewrigh et al. [20].

RESULTS AND DISCUSSION

After validation of numerical procedure, the results of numerical simulations for comprehensive thermo-hydrodynamic analysis of turbulent natural convection in a CPC cavity with an installed glass sheet are presented in this section. The contours of velocity magnitude with the streamline plots in free convection airflow are depicted in Figure 5 for clean CPC ($a=0$). The airflow after initialization from the pure conduction mode appears in a unicellular recirculated zone in the cavity of solar collector. The buoyant force near the high-temperature absorber surface pushes the working gas towards the cold glass cover, where the cooling effect of this element causes a downward streamline near the left sidewall. Consequently, a main recirculated cell lying in the central zone of cavity takes place because of the buoyancy force, with some small recirculated zones adjacent to the corners. The regions with higher velocity are seen near to the middle point of each boundary surface (including glass cover, sidewalls, and absorber) and an almost stagnant condition governs at the central zone of cavity.

A series of velocity magnitude contours at different lengths of glass sheet including the clean CPC are plotted in Figure 6. By installing the separating glass sheet, the absorber surface is kept away from the convective recirculated airflow. It leads to a considerable decrease in

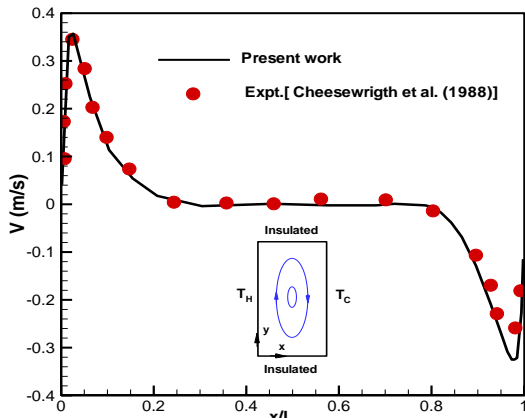


Figure 4. Air velocity distribution across the mid-line of cavity

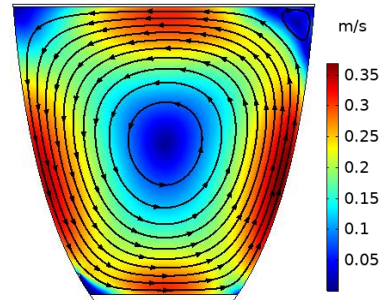


Figure 5. Streamline plots in clean CPC

the air velocity as it shown in Figure 6. This is due to the protection effect of glass sheet from convection heat transfer between the buoyant flow and absorber surface, that finally resulted in a lower air flow rate inside the recirculated zone, such that this behavior is enhanced as the length of glass sheet increases from 0.1 m to 0.3 m, after which no variation in thermal behavior was observed from numerical findings. It should be noted that the numerical results for the test cases with $a > 0.3$ m is not reported here for space saving.

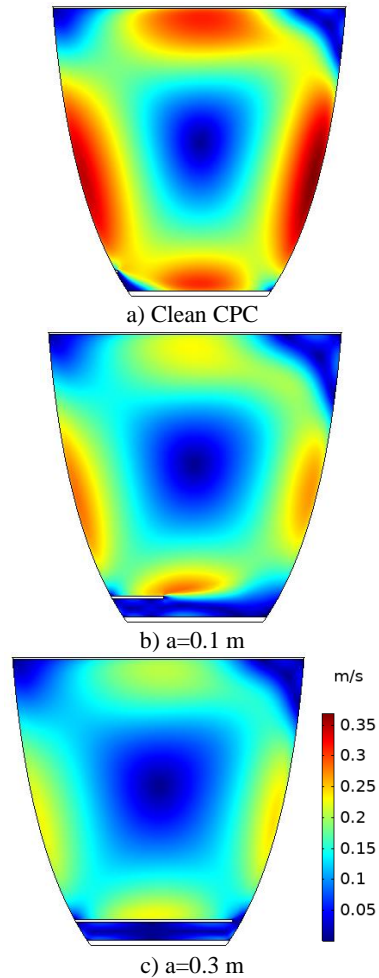


Figure 6. Velocity magnitude contours

The streamline plots of the natural convection airflow in CPCs with separating glass sheets are illustrated in Figure 7 for two different lengths. As seen, the absorber surface is kept away from the main recirculated zone, such that in the case of using a long separator with the length of $a=0.3$ m, the air gap between the glass sheet and absorber is almost at stagnant condition, in which the only mechanism of heat transfer is conduction. In other words, the free convection airflow adjacent to the absorber is completely damped by the long separator, while this process partially takes place by the short one ($a=0.1$ m).

The temperature contours inside the cavity for two different test cases with glass sheets and also for clean CPC are depicted in Figure 8. As seen, heat propagation from the absorber toward the natural airflow is prevented well by the glass sheet, especially in the case of $a=0.3$ m. This behavior causes higher temperature for the absorber and consequently, a higher rate of heat transfer from this element into the working fluid flow from the lower side. Also, the effect of separator in lowering the temperature of main recirculated flow inside the central region of cavity can be seen. This behavior decreases the glass cover temperature and finally leads to a lower rate of heat loss from this element.

The variation of air pressure inside the cavity is studied by plotting the pressure contours in clean CPC and under the presence of short and long glass sheets in Figure 9. The high-pressure regions near the absorber and low-pressure zone adjacent to the glass cover are shown in this figure. This pressure pattern comes from the

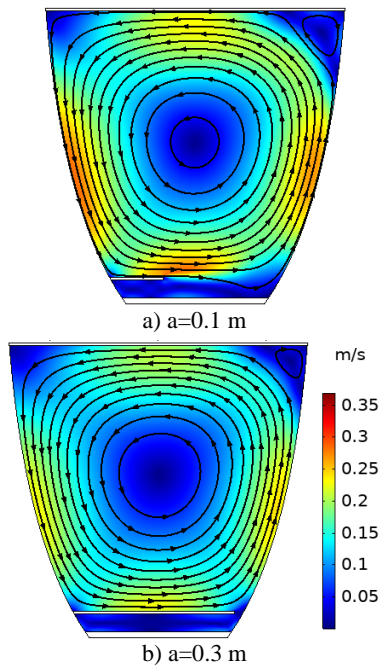


Figure 7. Streamline plots inside the CPCs with separating glass sheet

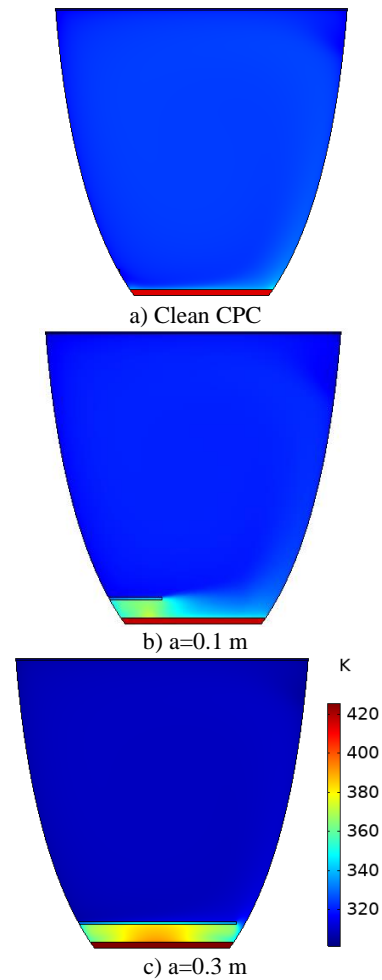


Figure 8. Air temperature contours inside the CPC

buoyancy forces and density gradient that finally lead to free convection airflow inside the CPC. Comparison between three test cases shows that the air pressure pattern is not much affected by the presence of glass sheet and only the high-pressure region is extended up to the upper side of glass sheet in cases Figures 9b and 9c.

To examine the effect of separating glass sheet on thermal characteristics of CPC, the temperature distributions along with the glass cover, right side wall, and absorber surface are drawn in Figure 10. Two different lengths are considered for the glass sheet in simulations, including the clean CPC. Figure 10a shows the low temperature at the two ends of the glass cover, while the maximum temperature takes place near the right end. This is due to the main recirculated zone that rotates with counterclockwise sense inside the cavity. If one compares the curves plotted in Figure 10a with each other, the positive effect of glass sheet in lowering the temperature of glass cover can be seen. The same behavior is also observed in Figure 10b for the side wall temperature. It should be mentioned that decreasing in glass cover and side walls temperatures leads to less heat

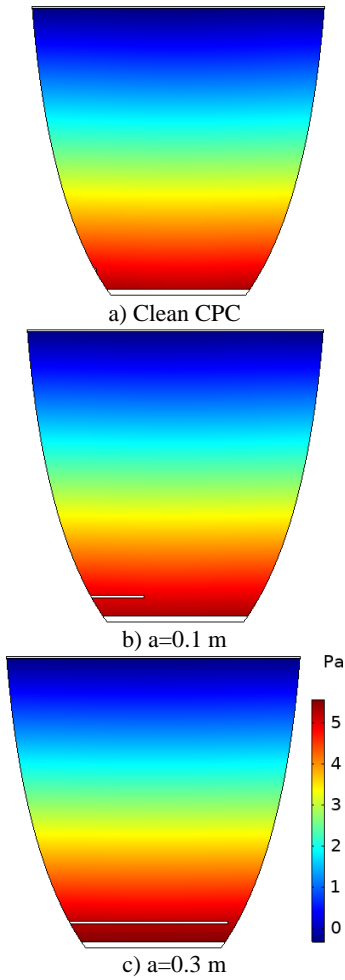


Figure 9. Pressure contours

loss and higher performance of CPC. The absorber distribution plotted in Figure 10c demonstrates an almost isotherm condition for all of the test cases, such that about 2.7% temperature increase takes place on the absorber because of using separating glass sheet with the length of $a=0.3$ m. It should be recalled that the long separating glass sheet completely damps the air convective flow adjacent to the absorber, such that this process is partially done in the case of using the short glass sheet.

The positive effect of glass sheet in improving the performance of CPC can be seen from Figure 11, in which the variation of heat flux on the lower surface of absorber, where it is in contact with the forced convection of the working fluid is depicted. For all of the test cases, uniform heat flux takes place on the absorber and a considerable increasing about 17% in the absorber heat flux can be computed due to employing the glass sheet in the construction of solar collector.

One of an important factors that has a great effect on the thermal performance of CPC is the temperature of working fluid which is in convection heat transfer with absorber via its lower surface. To study the effect of this

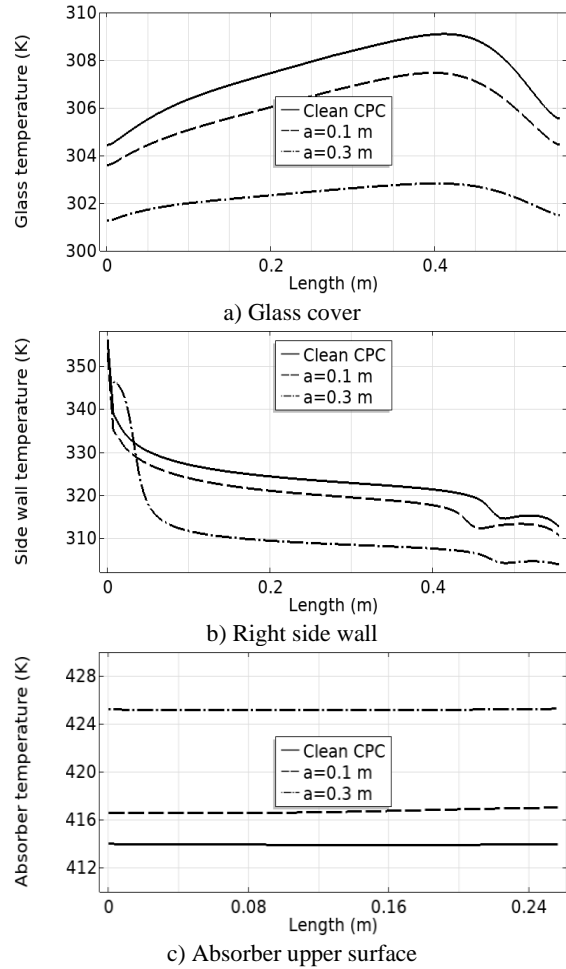


Figure 10. Temperature distribution

parameter, the air temperature contours in a CPC with a long separating glass sheet and for four different values of T_0 are drawn in Figure 12. This figure shows that the whole region inside the CPC is affected by the working fluid temperature, such that the air temperature inside the cavity of collector increases as T_{wf} gets higher values, and this behavior is enhanced for the air layer between the absorber and separating glass sheet.

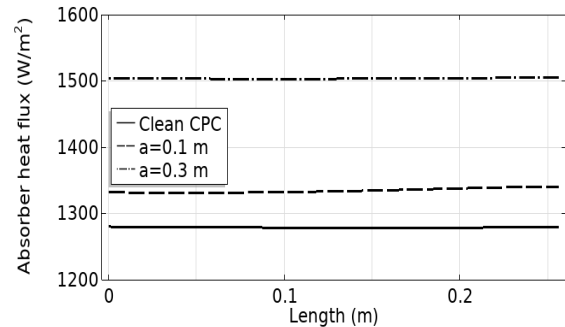


Figure 11. Distribution of heat flux along the lower surface of absorber

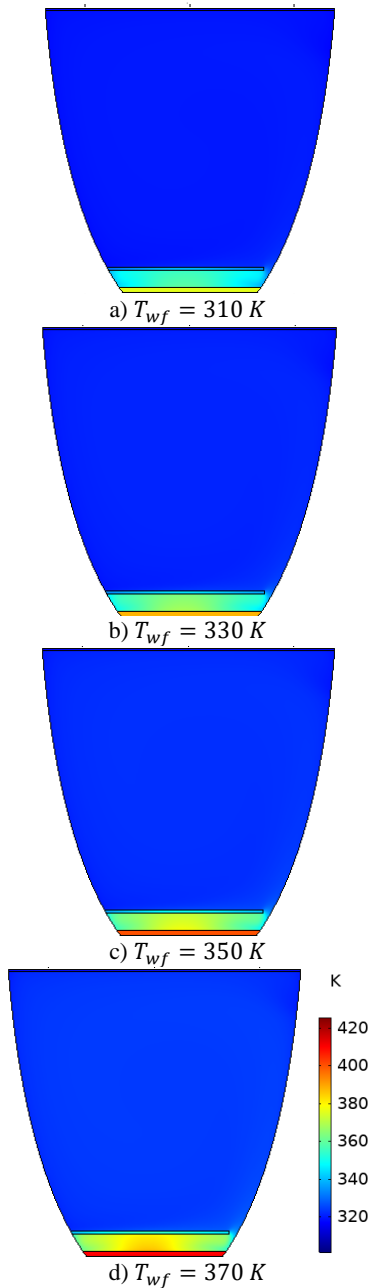


Figure 12. Temperature contours inside the CPC at different working fluid temperature ($a=0.3\text{ m}$)

The contours of velocity magnitude along with the vector field of turbulent free convection airflow are plotted in Figure 13, at four different values of the working fluid temperature. This figure reveals the great effect of T_{wf} on the hydrodynamic characteristics of CPC, such that increasing in working fluid temperature leads to a higher rate of flow vortices in the recirculated zone. At this condition, the rate of convective heat transfer between the airflow and glass cover gets higher values and due to increase in the rate of heat loss, the CPC efficiency decreases.

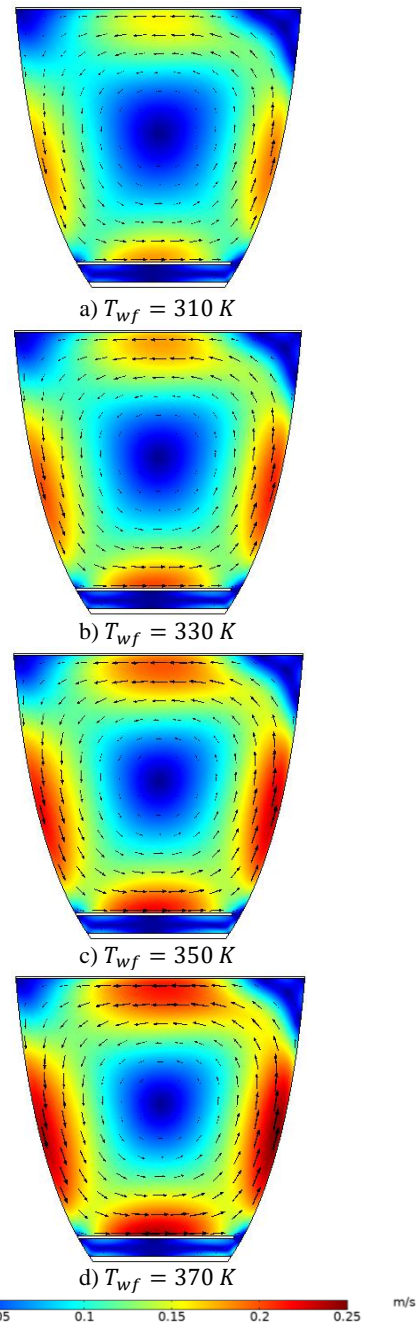


Figure 13. Vector fields at different values of the working fluid temperature ($a=0.3\text{ m}$)

The temperature variations along the vertical centerline of CPC, from the lower surface of absorber up to the top of glass cover are plotted in Figure 14 for different values of the working fluid temperature. As shown, the air layer between the absorber and glass sheet is a high- temperature region and a sudden temperature decrease happens across the glass sheet, after which an isotherm condition is seen inside the main recirculated zone. So, the CPC cavity is divided into high-temperature and low-temperature sub-domains by

employing the glass sheet. Figure 14 shows that the working fluid temperature has a great effect on the absorber temperature and also on the temperature of air gap between this element and the glass sheet. To investigate more about the effect of working fluid temperature, the distribution of absorber heat flux on its lower surface, where this element is in convection heat transfer with the working fluid, are plotted in Figure 15 at different values of T_0 . This figure again shows almost uniform heat flux distribution along with the absorber, such that there is a considerable decrease in the amount of this parameter as the working fluid gets higher temperatures. So, the performance of CPCs will be improved by decreasing in the temperature of working fluid.

The temperature variations along the vertical centerline of CPC, from the lower surface of absorber up to the top of glass cover are plotted in Figure 14 for different values of the working fluid temperature. As shown, the air layer between the absorber and glass sheet is a high temperature region and a sudden temperature decrease happens across the glass sheet, after which an isotherm condition is seen inside the main recirculated zone. On the other word, the CPC cavity is divided into high temperature and low temperature sub-domains by employing the glass sheet. Figure 14 shows that the working fluid temperature has a great effect on the absorber temperature and also on the temperature of air gap between this element and the glass sheet. To study more about the effect of working fluid temperature, the distribution of absorber heat flux on its lower surface, where this element is in convection heat transfer with the working fluid, are plotted in Figure 15 at different values of T_0 . This figure again shows almost uniform heat flux distribution along the absorber, such that there is a considerable decrease in the amount of this parameter as the working fluid gets higher temperatures. So, the performance of CPCs will be improved by decreasing in the temperature of working fluid.

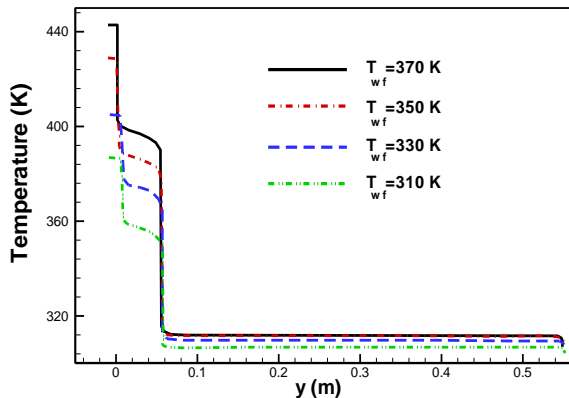


Figure 14. Air temperature distribution along the CPC centerline at different working fluid temperature, a=0.3 m

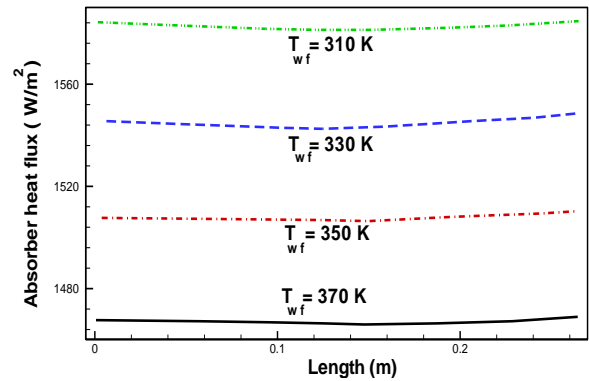


Figure 15. Absorber surface heat flux at different working fluid temperature, a=0.3 m

To examine the positive effect of separating glass sheet on the performance of solar collectors, the efficiency of CPC at several test cases with different lengths of the glass sheet and at various working fluid temperatures are computed as follows and plotted in Figure 16.

$$\eta = \frac{\text{Rate of heat transfer to the working fluid}}{q_{\text{sun}} \cdot A_{\text{Aperture}}} \quad (7)$$

This figure reveals an increasing trend for efficiency with the length of glass sheet, such that for the studied test cases, the maximum efficiency is achieved at the length of 0.34 m, after which the efficiency increase has vanished because of the dominance of conduction mode of heat transfer and the complete damping of convection inside the air gap between the absorber and separating glass sheet. The maximum percent of efficiency increase according to the computations of Figure 16 is about 24%, which can be considered as a great improvement in the performance of CPCs. Also, a comparison between the curves plotted in Figure 16 reveals higher efficiencies for the CPCs with lower working fluid temperature.

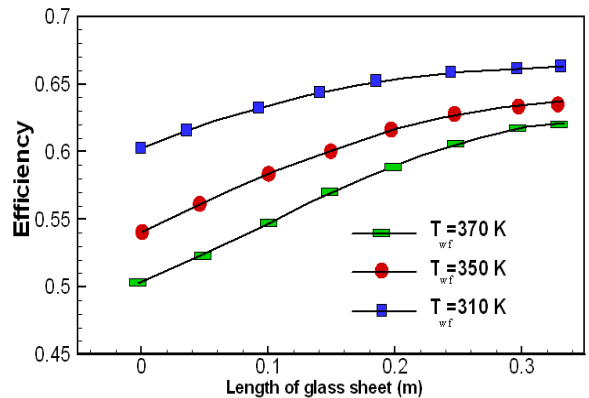


Figure 16. Variation of CPC efficiency with the length of glass sheet

CONCLUSION

In this work, a new and simple technique for improving the thermal performance of parabolic collectors is proposed by theoretical analysis. Numerical findings revealed that the installation of a separating thin glass sheet near to the absorber damps the free convection air flow adjacent to the heated surface and causes a considerable decrease in the rate of heat loss from the thermal system. Comparison between the present findings with experimental data published in research papers showed very good consistency. The set of flow equations for free convection turbulent airflow and conduction equations inside the solid elements including the absorber plate, separating glass sheet and glass cover were solved numerically by the FEM. Numerical results showed about 24% increase in the value of thermal efficiency under the presence of glass sheet near to the absorber plate.

REFERENCES

- Solaymani, S., 2021. A Review on Energy and Renewable Energy Policies in Iran. *Sustainability*, 13(7328), pp.1–23. Doi: 10.3390/su13137328
- Bolígán Rojas, G., Lorenzo Ávila Rondon, R., and Carolina Meléndez Gurrola, A., 2018. Mechanical Engineering Design Theory Framework for Solar Desalination Processes: A Review and Meta-Analysis. *Iranian (Iranica) Journal of Energy and Environment*, 9(2), pp.137–14. Doi: 10.5829/IJEE.2018.09.02.09
- Premkumar, S., Ramanarasimha, K., and Prakash, E.S., 2018. Design and Development of Solar Crop Dryer Integrated with Oil Bath. *Iranian (Iranica) Journal of Energy and Environment*, 9(4), pp.277–283. Doi: 10.5829/IJEE.2018.09.04.08
- Junfeng, L., and Runqing, H., 2005. Solar thermal in China. *Refocus*, 6(5), pp.25–27. Doi: 10.1016/S1471-0846(05)70454-6
- Xu, D., and Qu, M., 2013. Compound Parabolic Concentrators in Solar Thermal Applications: A Review. In: ASME 2013 7th International Conference on Energy Sustainability. American Society of Mechanical Engineers
- Francesconi, M., Caposciutti, G., and Antonelli, M., 2018. CFD optimization of CPC solar collectors. *Energy Procedia*, 148, pp.551–558. Doi: 10.1016/j.egypro.2018.08.138
- Reichl, C., Hengstberger, F., and Zauner, C., 2013. Heat transfer mechanisms in a compound parabolic concentrator: Comparison of computational fluid dynamics simulations to particle image velocimetry and local temperature measurements. *Solar Energy*, 97, pp.436–446. Doi: 10.1016/j.solener.2013.09.003
- Eames, P.C., Norton, B., and Kothdiwala, A.F., 1996. The state of the art in modelling line-axis concentrating solar energy collectors. *Renewable Energy*, 9(1–4), pp.562–567. Doi: 10.1016/0960-1481(96)88352-2
- Chew, T.C., Tay, A.O., and Wijesundera, N.E., 1989. A Numerical Study of the Natural Convection in CPC Solar Collector Cavities with Tubular Absorbers. *Journal of Solar Energy Engineering*, 111(1), pp.16–23. Doi: 10.1115/1.3268281
- Antonelli, M., Francesconi, M., Di Marco, P., and Desideri, U., 2016. Analysis of heat transfer in different CPC solar collectors: A CFD approach. *Applied Thermal Engineering*, 101, pp.479–489. Doi: 10.1016/j.applthermaleng.2015.12.033
- Milani Shirvan, K., Mamourian, M., Mirzakhani, S., Rahimi, A.B., and Ellahi, R., 2017. Numerical study of surface radiation and combined natural convection heat transfer in a solar cavity receiver. *International Journal of Numerical Methods for Heat & Fluid Flow*, 27(10), pp.2385–2399. Doi: 10.1108/HFF-10-2016-0419
- Akhter, J., Gilani, S.I., Al-Kayiem, H.H., Mehmood, M., Ali, M., Ullah, B., Alam, M.A., and Masood, F., 2021. Experimental Investigation of a Medium Temperature Single-Phase Thermosyphon in an Evacuated Tube Receiver Coupled With Compound Parabolic Concentrator. *Frontiers in Energy Research*, 19(9). Doi: 10.3389/fenrg.2021.754546
- Jiang, Yu, Yang, Li, Wang, Lund, and Zhang, 2020. A Review of the Compound Parabolic Concentrator (CPC) with a Tubular Absorber. *Energies*, 13(3), pp.695. Doi: 10.3390/en13030695
- Gandjalikhan Nassab, S.A., and Moein Addini, M., 2021. Effect of Radiative Filling Gas in Compound Parabolic Solar Energy Collectors. *Iranian (Iranica) Journal of Energy and Environment*, 12(3), pp.181–191. Doi: 10.5829/IJEE.2021.12.03.01
- Ma, G., Yin, Z., Liu, X., Qi, J., and Dai, Y., 2021. Developments of CPC solar evacuated glass tube collector with a novel selective coating. *Solar Energy*, 220, pp.1120–1129. Doi: 10.1016/j.solener.2020.08.052
- Tang, L.H., Chu, W.X., Ahmed, N., and Zeng, M., 2016. A new configuration of winglet longitudinal vortex generator to enhance heat transfer in a rectangular channel. *Applied Thermal Engineering*, 104, pp.74–84. Doi: 10.1016/j.applthermaleng.2016.05.056
- Singh, A.P., Akshayveer, Kumar, A., and Singh, O.P., 2019. Designs for high flow natural convection solar air heaters. *Solar Energy*, 193, pp.724–737. Doi: 10.1016/j.solener.2019.10.010
- Lauder, B.E., and Spalding, D.B., 1974. The numerical computation of turbulent flows. *Computer Methods in Applied Mechanics and Engineering*, 3(2), pp.269–289. Doi: 10.1016/0045-7825(74)90029-2
- Singh, S., 2017. Performance evaluation of a novel solar air heater with arched absorber plate. *Renewable Energy*, 114, pp.879–886. Doi: 10.1016/j.renene.2017.07.109
- Cheesewright, R., 1986. Experimental Data for Validation of Computer codes for the Prediction of Two-Dimensional Buoyant Cavity Flows. In: ASME Winter Annual Meeting, 1986. pp 75–81

COPYRIGHTS

©2021 The author(s). This is an open access article distributed under the terms of the Creative Commons Attribution (CC BY 4.0), which permits unrestricted use, distribution, and reproduction in any medium, as long as the original authors and source are cited. No permission is required from the authors or the publishers.



Persian Abstract

چکیده

در این مقاله نقش یک جداکننده شیشه‌ای نازک به منظور کاهش نرخ افت حرارتی و افزایش کارایی کلکتورهای خورشیدی مرکب سهموی مورد تجزیه و تحلیل قرار گرفته است. این جداکننده در نزدیکی صفحه جاذب و بر روی دیواره جانبی کلکتور نصب شده و ناحیه داغ نزدیک صفحه جاذب را از جریان چرخشی هوا در داخل محفظه کلکتور دور نگه می‌دارد. در شبیه‌سازی مسئله باروش المان محدود، معادلات حاکم برای جریان جابجایی آزاد در حالت متلاطم شامل پیوستگی، ممنتم وانرژی توسط نرم‌افزار کامسول حل عددی شده است و جهت محاسبه تنش و شار حرارتی آشفته مدل شناخته شده بکار گرفته شده است. نتایج بدست آمده گواه بر نقش موثر جداکننده شیشه‌ای بر عملکرد کلکتور را نشان داده به طوری که در موارد شبیه‌سازی شده یافته‌های عددی حاکی بر افزایش ۲۴ درصدی راندمان حرارتی کلکتور بوده است. مقایسه بین نتایج حاصل از مطالعه عددی حاضر و داده‌های تجربی، موید صحت روش بکارگرفته شده می‌باشد.
